

Exploring QUIC Dynamics: A Large-Scale Dataset for Encrypted Traffic Analysis

Barak Gahtan*

Robert J. Shahla*

barakgahtan@cs.technion.ac.il

shahlarobert@cs.technion.ac.il

Computer Science Department ,
Technion
Haifa, Israel

Alex M. Bronstein

Department of Computer Science,
Technion

Haifa, Israel

bron@cs.technion.ac.il

Reuven Cohen

Department of Computer Science,
Technion

Haifa, Israel

rcohen@cs.technion.ac.il

Abstract

QUIC, an increasingly adopted transport protocol, addresses limitations of TCP by offering improved security, performance, and features such as stream multiplexing and connection migration. However, these enhancements also introduce challenges for network operators in monitoring and analyzing web traffic, especially due to QUIC’s encryption. Existing datasets are inadequate—they are often outdated, lack diversity, anonymize critical information, or exclude essential features like SSL keys—limiting comprehensive research and development in this area. We introduce VisQUIC, a publicly available dataset of over 100,000 labeled QUIC traces with corresponding SSL keys, collected from more than 40,000 websites over four months. By generating visual representations of the traces, we facilitate advanced machine learning (ML) applications and in-depth analysis of encrypted QUIC traffic. To demonstrate the dataset’s potential, we estimate the number of HTTP/3 request-response pairs in a QUIC connection using only encrypted traffic, achieving up to 92% accuracy. This estimation provides insights into server behavior, client-server interactions, and connection load—crucial for tasks like load balancing and intrusion detection. Our dataset enables comprehensive studies on QUIC and HTTP/3 protocols and supports the development of tools for encrypted traffic analysis.

1 Introduction

Monitoring and analyzing web traffic is crucial for network operators to ensure security, optimize performance, and understand user behavior. The rapid adoption of Quick UDP Internet Connections (QUIC) [12] as a transport protocol offers significant enhancements over traditional TCP, including improved security, performance, stream multiplexing, and connection migration. However, these advancements introduce challenges for network monitoring and analysis, particularly due to QUIC’s encryption.

Traditional methods of traffic analysis are less effective with QUIC because encryption obscures packet contents, necessitating innovative approaches to manage network performance and analyze effects on latency, error rates, and congestion control. Addressing these challenges requires innovative datasets that reflect the encrypted nature of QUIC traffic while enabling meaningful analysis through modern techniques. Consequently, the development of a comprehensive and diverse dataset of QUIC traffic is essential for thorough research.

On one hand, there are very few datasets of network traces due to privacy concerns. On the other hand, those that are available are heavily anonymized or do not contain all the necessary information, variety and diversity [4, 16, 21]. Moreover, the continuous evolution of protocols such as QUIC and changes in network behaviors necessitate regularly updated benchmark datasets.

Our Contributions: In this paper, we address these challenges by introducing *VisQUIC*, a labeled dataset comprising over 100,000 QUIC traces collected from more than 44,000 websites over a four-month period from various vantage points using a page-request workload. The dataset considers the case of an observer passively monitoring the channel between a QUIC client and server, seeing encrypted data packets sent in both directions. Our contributions are:

- (1) **Dataset:** We release a large-scale, real-world dataset of QUIC traffic, unprecedented in scale and richness, which includes corresponding SSL keys to enable decryption and detailed analysis.
- (2) **Image Generation Methodology:** We propose a novel method for transforming QUIC traffic traces into learnable RGB images.
- (3) **Use Case Demonstration:** We demonstrate the dataset’s potential by presenting a baseline algorithm to estimate the number of HTTP/3 [3] request-response pairs in encrypted QUIC connections, which is critical for applications like HTTP/3 load balancing and detecting HTTP/3 flood attacks [5].

*Both authors contributed equally to this research.

The *VisQUIC* dataset results in over seven million labeled images, using two different window lengths, providing a rich resource for ML tasks in network analysis. By making this dataset publicly available ¹, we facilitate comprehensive research on the behavior of HTTP/3 and QUIC, enabling advancements in network monitoring and security.

The rest of this paper is organized as follows: Section 2 reviews existing datasets, Section 3 describes the dataset and the image generation process. Section 4 defines the problem settings and presents an algorithm for estimating the number of HTTP/3 responses in QUIC connections. Section 5 concludes the paper.

2 Available Datasets

In this section, we analyze publicly available datasets related to QUIC traffic to highlight their shortcomings and demonstrate the need for a comprehensive and reliable dataset like *VisQUIC*.

The study of QUIC [1] and its impact on network traffic has gained significant traction due to its potential to enhance web performance and security. However, research in this area is limited by the absence of comprehensive datasets that provide detailed insights into QUIC traffic. Existing datasets often lack crucial information such as full packet payloads, SSL keys, or detailed metadata, making it challenging to perform in-depth analyses, especially given QUIC’s encryption.

Datasets focusing on TLS over TCP traffic are inadequate for QUIC studies due to fundamental protocol differences. QUIC operates over UDP, integrating encryption directly into the transport layer and combining features of TLS and TCP into a single protocol. Additionally, QUIC introduces new features such as 0-RTT connection establishment, stream multiplexing, and seamless connection migration, which are not present in TLS over TCP. Moreover, QUIC encrypts headers that are typically accessible in TLS over TCP traffic, making traditional analysis methods ineffective. Given that browsers like Google Chrome, holding approximately 63% of the market share [22], have widely adopted QUIC and HTTP/3, a significant portion of internet traffic now uses QUIC. This highlights the need for dedicated QUIC datasets with decryptable traffic and detailed protocol metadata to study QUIC’s unique features.

The **CESNET-QUIC22** dataset [16] comprises QUIC traffic collected from backbone lines of a large Internet service provider. It contains over 153 million connections and 102 service labels from one month of traffic, offering a degree of diversity. However, it has significant limitations. First, metadata such as direction, inter-packet time, and size are provided only for the first 30 packets of each connection, limiting research on complete connections. Second, the dataset does

not include HTTP/3 protocol information, making it inadequate for studies focusing on HTTP/3 over QUIC. Without details about HTTP/3, analysis of application-layer behaviors and performance characteristics are limited. Furthermore, the dataset lacks SSL keys and full payloads, making decryption and detailed examination of encrypted traffic impossible. This absence prevents in-depth security analysis and understanding of QUIC’s encrypted payload characteristics.

The dataset provided by [21] is a combined dataset of TCP and QUIC traces. It is collected from three different VPN gateways worldwide. While this dataset offers geographical diversity using a VPN, it has several drawbacks. Collecting traces from multiple VPN gateways can introduce inconsistencies due to varying network conditions, which complicates fair comparisons between traces and web servers. Differences in latency, packet loss, and routing paths can affect the observed traffic patterns, making it challenging to isolate variables for analysis.

The **CAIDA** dataset [4] comprises traffic traces collected from monitors on commercial backbone links. While extensive in scope, it has critical limitations that affect its usefulness for QUIC studies. The payload is removed from all packets, retaining only header information up to the transport layer. This prevents any analysis involving payload content or encryption features, which are essential for studying QUIC’s encrypted traffic and application-layer protocols like HTTP/3. Moreover, the dataset is not tailored to QUIC traffic and lacks details necessary for QUIC and HTTP/3 studies.

The limitations of existing datasets underscore the necessity for a comprehensive QUIC dataset that addresses these gaps. A dataset with full packet captures, payloads, and SSL keys is essential for detailed analysis of QUIC’s encrypted traffic and HTTP/3 protocol data, enabling in-depth studies on protocol behavior, security features, and performance.

Collecting traces from various vantage points ensures consistency and fairness in comparisons by minimizing variables introduced by differing network conditions. This approach allows for accurate assessments of server behaviors and protocol performance across different web servers.

By reflecting current network behaviors with data collected from a wide range of websites over an extended period, the dataset remains up-to-date and diverse, enhancing the generalizability of research findings. Our proposed *VisQUIC* dataset meets these needs by offering over 100,000 QUIC traces with corresponding SSL keys, collected from more than 44,000 websites over a four-month period, from various vantage points. Additionally, we provide image representations of the traces, enabling advanced ML analysis. This dataset empowers researchers to conduct comprehensive studies on QUIC and HTTP/3, overcoming the limitations of existing datasets.

¹At: <https://github.com/robshahla/VisQUIC>

3 VisQUIC

In this section, we introduce the *VisQUIC* dataset, a comprehensive collection of QUIC traffic traces accompanied by SSL keys and image representations, designed to facilitate advanced research in network analysis and ML.

3.1 Dataset Collection and Generation

The process starts with HTTP/3 [3] GET requests that are generated to various web servers that support HTTP/3, each hosting multiple websites. Requests are issued for up to 26,000 different websites per web server. Headless Chrome [6] is used in incognito mode with the application cache disabled, and the websites are requested sequentially, resulting in a web-page request workload. Table 1 displays the exact numbers for each web server and more detailed statistics broken down per web server for each class are provided in Appendix A.3. The generated network traffic traces are captured using Tshark [18] in packet capture (PCAP) format. These traces include only QUIC packets and cover the duration of the website request. For each PCAP file the corresponding SSL keys are stored to be used later to decrypt the traffic. The SSL keys are also provided in the dataset’s materials.

3.2 Image Generation Technique

To transform the network traffic data into a format suitable for ML models, we converted the captured traces into images. This process involves representing features such as packet arrival times, packet sizes, packet density, and packet directions as visual elements in an image. The use of images enhances pattern recognition abilities [8, 11, 20, 23, 24], allowing deep learning models to identify intricate patterns in network traffic.

Figure 1 illustrates the steps involved in constructing an image from a trace:

- (1) **Data Extraction:** Collect packet metadata including arrival time, length, and direction (client-to-server and server-to-client).
- (2) **Time and Length Binning:** Divide the time span of the trace into M equispaced time bins and the packet lengths into N bins.
- (3) **Histogram Construction:** Count the number of packets in each bin based on time and length, separately for each direction.
- (4) **Image Creation:** Map the histogram counts to pixel intensities in an RGB image, with the red channel representing server-to-client packets and the green channel representing client-to-server packets. The blue channel remains unused.

This technique extends the FlowPic method [20] by incorporating directional information and configurable parameters such as window length and resolution. FlowPic’s

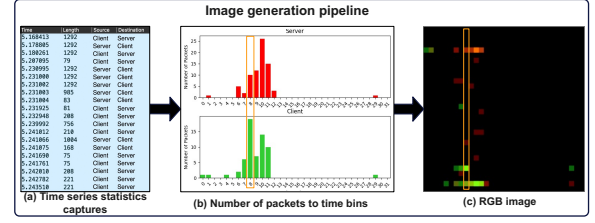


Figure 1: Construction of an image from a QUIC trace. Packet metadata is binned by time and length, and mapped to pixel intensities resulting in an RGB image.

single-channel approach, while providing a general traffic overview, is insufficient in the context of QUIC. In QUIC, distinguishing between client-to-server and server-to-client traffic is critical due to the multiplexed nature of HTTP/3 requests and responses. Furthermore, QUIC’s inherent complexity—stemming from stream multiplexing and independent packet handling—necessitates a more detailed examination of traffic directions. For those reasons, we introduce a separate channel for each direction between a client and a server, a density factor for the packets’ count in a given window, and a configurable number of bins.

Images whose class labels were above 20 responses were not part of the training or evaluation for estimating the number of responses in a QUIC connection, due to their rarity in the data. Besides that, the raw data contains all of the data, unfiltered. Preprocessing was done by filtering out packets that are not QUIC packets. Furthermore, a large number of images were identical, and all of the duplicate images were removed. Before the filtering there was 21, 100, 925 images, and after there was 5, 040, 459 images. We upload the full dataset including the duplicates.²

The *VisQUIC* dataset includes three main components: trace data, image data, and labels. The **trace data** comprises over 100,000 QUIC traces collected from more than 44,000 websites. For each trace, the corresponding SSL keys are provided to enable decryption, allowing in-depth analysis of the encrypted traffic. The **image data** consists of over seven million images generated from the traces. These images are created using two different window lengths, $T = 0.1$ seconds and $T = 0.3$ seconds, capturing network traffic at varying temporal resolutions. The images have a resolution of $M = N = 32$, which balances the level of detail captured with computational efficiency, making them suitable for ML applications. Each image can be associated with **labels**, such as the number of HTTP/3 requests or responses observed during the captured window. These labels are derived using the SSL keys to decrypt the traces and extract relevant

²The captured traces, images, and code will be available upon the paper’s acceptance using a GitHub link.

Table 1: Summary statistics of QUIC traces and the number of images per dataset for each web server.

Web Server	Websites	Traces	$T = 0.1$	$T = 0.3$
youtube	399	2,109	139,889	54,659
semrush	1,785	9,489	474,716	221,477
discord	527	7,271	623,823	235,248
instagram	3	207	17,003	7,112
mercedes-benz	46	66	9,987	2,740
bleacherreport	1,798	8,497	781,915	331,530
nicelocal	1,744	1,666	148,254	48,900
facebook	13	672	25,919	10,988
pcmag	5,592	13,921	1,183,717	385,797
logitech	177	728	56,792	28,580
google	1,341	2,149	81,293	29,068
cdnetworks	902	2,275	207,604	85,707
independent	3,340	3,453	176,768	68,480
cloudflare	26,738	44,700	1,347,766	341,488
jetbrains	35	1,096	34,934	18,470
pinterest	43	238	6,465	2,360
wiggle	4	0	0	0
cnn	27	2,127	91,321	59,671

metadata. This labeling enables the dataset to be used for supervised learning tasks, facilitating research in network traffic analysis and ML. Table 1 present *VisQUIC*'s characteristics.

3.3 Discussion

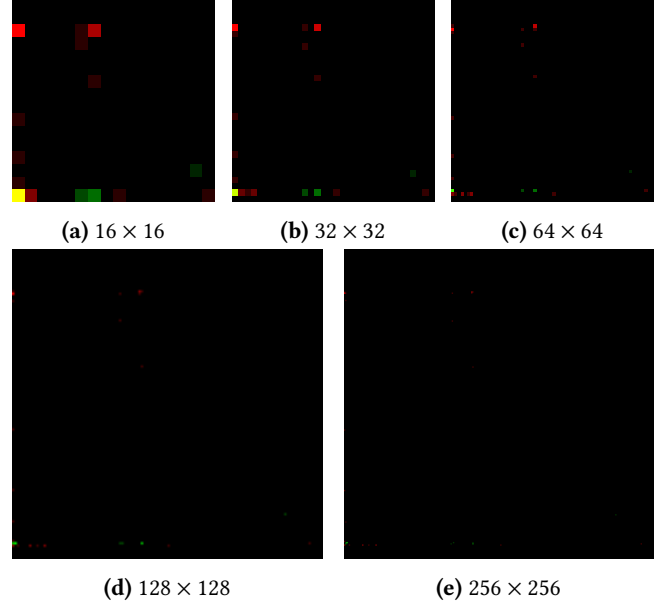
When generating images for the *VisQUIC* dataset, the choice of parameters significantly influences their effectiveness for analysis.

Window Length (T): The window length determines the temporal span of each image and affects data granularity. Shorter windows capture detailed interactions but increase computational demands due to more images, while longer windows provide an aggregated view, reducing image count but potentially obscuring fine-grained details.

Image Resolution: Resolution balances detail and computational efficiency. Higher resolutions capture finer features but increase resource requirements. The resolution should align with the analysis goals and computational constraints.

Normalization Approach: Normalization impacts outcomes by scaling packet counts. Per-window normalization highlights short-term variations, aiding detection of subtle differences, while per-trace normalization captures long-term patterns but may reduce sensitivity to short-term fluctuations. The choice depends on specific analysis needs.

Choosing Image Parameters: Figure 2 illustrates the effect of resolution on image representation. At lower resolutions (e.g., Figure 2(a)), a yellow pixel combines packets from both directions (red and green channels). Increasing resolution (Figures 2(b) and 2(c)) splits these into separate red or green pixels, providing finer granularity and more detailed insights into packet interactions.

**Figure 2: Five example images of QUIC flows using $T = 0.1$ -second windows with different pixel levels.**

3.4 Potential Applications of the Dataset

VisQUIC offers significant value in both networking and ML domains by enabling the analysis of QUIC and HTTP/3 behavior under real-world conditions. Researchers can leverage the comprehensive data provided by the dataset to develop tools and methodologies that enhance network performance and advance ML techniques.

From a **networking** perspective, the dataset assists in detecting DDoS attacks and traffic anomalies, which is crucial for maintaining network security and reliability. It enables the examination of symmetric and asymmetric flows to identify application types, aiding in effective traffic management. Additionally, estimating round-trip times (RTT) helps ISPs monitor their network performance and manage it accordingly, and lastly estimating the number of responses in a connection a load balancer. The dataset also facilitates studies on encrypted traffic patterns, congestion control mechanisms, and protocol performance, which are essential for understanding and enhancing modern network communications.

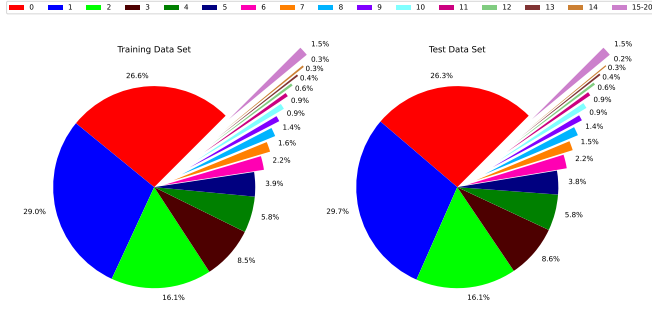


Figure 3: Response distribution for training and evaluation datasets with a $T = 0.1$ -second sliding window.

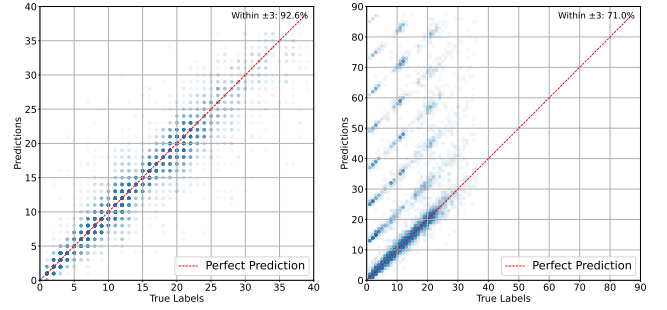
From an ML perspective, the dataset allows for the exploration of image-based representations of network traffic for classification and regression tasks. Researchers can study the effects of different image resolutions on deep learning model performance, providing insights into optimizing models for various applications. The dataset supports the investigation of methods for handling significant class imbalances and ordinal regression tasks, addressing common challenges in ML with real-world data. Furthermore, it offers opportunities to develop new loss functions tailored to the unique structure of the dataset.

Dataset Accessibility *VisQUIC* is made publicly available to the research community, providing a valuable resource for advancing studies in QUIC, HTTP/3, and related areas. Details on accessing the dataset are provided on [DatasetWebsite/Repository] upon request.

4 Estimating the Number of HTTP/3 Responses in a QUIC Connection

We consider an observer who can see the encrypted QUIC packets transmitted between the client and the server. For each packet, the observer knows its direction, length, and observed time. Using this information, the QUIC traces can be converted into representative colored images suitable for training ML models. To convert the captured QUIC traces into time-series data, we use the sliding window technique Frank et al. [10], which requires two configurable parameters: the window length and the overlap between consecutive windows. These images enable use cases like estimating HTTP/3 responses to aid load balancing.

Estimating the number of HTTP/3 responses in a QUIC connection can assist a load balancer in making more informed decisions. By monitoring connections and estimating the number of responses within each connection, the load balancer can determine if a connection is considered heavy and adjust its decision on the selected server accordingly [19]. To evaluate the use of *VisQUIC*, we formulate



(a) Window length $T = 0.1$ -sec (b) Window length $T = 0.3$ -sec

Figure 4: Scatter plots demonstrating the predictive results, where each point represents the summed predictions of a trace compared to its true label, with transparency set to 0.05 to distinguish point density in overlapping areas.

estimating the number of responses in a QUIC connection as a discrete regression problem and evaluate it using images derived from the traces. The dataset can be split into two settings: when the web servers are known to the observer and when they are not. We provide an evaluation for the case when the web servers are known to the observer. Therefore, the training and evaluation phases are conducted exclusively on the QUIC traces pertaining to the web servers assumed at inference time, using an 80 : 20 train-test split to ensure out-of-sample evaluation.

This is not a classic classification task because misclassification errors depend on the distance between predicted and actual categories. For example, estimating an image with 17 responses as 16 is better than estimating it as 15 or 19. It is also not a standard regression task, as the target categories are discrete. To address this issue, we developed a dedicated loss function coupled with data augmentation that: (1) accounts for the imbalanced dataset derived from real-world QUIC traces, and (2) rewards the model for correctly predicting classes closer to the actual label over those that are farther away. Appendix A.1 explains the discrete regression loss function in more detail.

We present a quantitative evaluation of the proposed framework when the web servers are known to the observer, using a subset of the dataset not included in training. Models were trained and evaluated exclusively on the QUIC traces pertaining to the web servers assumed at inference time. Two different models were trained with window lengths of $T = 0.1$ and $T = 0.3$ seconds. Classes with labels less than or equal to 20 constitute 90% of the traces in the $T = 0.3$ -second window dataset and 95% in the $T = 0.1$ -second window dataset. Due to their scarcity, classes above 20 were excluded from the training and test sets. While both $T = 0.1$ - and

$T = 0.3$ -second sliding window datasets were created, we include only the response distribution for the $T = 0.1$ dataset in Figure 3 for brevity. The $T = 0.3$ dataset exhibits similar trends, with slight variations in the distribution due to the larger window size. Figure 3 shows the images distribution for the created images datasets.

To address class imbalance, we developed a dedicated loss function and implemented a data augmentation technique. A grid search was used to optimize loss function parameters α , β , and γ , with $\alpha \in 0.3, 0.5, 0.7$, $\beta \in 0.4, 0.6$, and $\gamma \in 1, 2, 3$. The optimal values, selected based on the lowest validation loss during training, were $\alpha = 0.7$, $\beta = 0.4$, and $\gamma = 2$ for $T = 0.3$ seconds, and $\gamma = 3$ for $T = 0.1$ seconds with the same α and β . Data augmentation was applied selectively to minority classes (values 10–20) since the 32×32 pixel grids, derived from QUIC traces, encode temporal dependencies that non-order-preserving modifications could disrupt. Therefore, we introduced minimal noise with a standard deviation of $\sigma = 2.55$ (1% of pixel value), preserving temporal integrity while enhancing model robustness and generalization [17]. Training was performed with a batch size of 64 images using the Adam optimizer [14] and the ReduceLROnPlateau learning rate scheduler, reducing the learning rate by 30% when a plateau was detected, with an early stopping technique.

The results presented are for estimating the total number of HTTP/3 responses in a complete trace. The images were fed sequentially through the trained models, whose predictions were summed and compared to the sum of the trace’s true labels. Figure 4 shows prediction results using the evaluation traces with the $T = 0.1$ - and $T = 0.3$ -second subdivisions.

In these scatter plots, the parameter θ , ranging between 0 and 1, modulates the transparency of the points. We set θ to 0.05 to enhance visual distinction between areas of high and low point density among the roughly 12,000 data points. Each point represents the summed predictions over the images of a trace compared to its true label. For example, if a trace is composed of five non-overlapping images with true labels 1, 0, 2, 4, and 1 (totaling 8), and the model’s predictions are 1, 0, 3, 4, and 1 (totaling 9), the trace is represented at the point (8, 9) in the plot. Overlapping points become darker due to the transparency setting.

Additionally, we introduce a Cumulative Accuracy Profile (CAP) metric, which provides a refined measure of classification accuracy by incorporating a tolerance level for each prediction. Unlike traditional metrics such as confusion matrices that require exact matches between predicted and true labels, CAP allows for a specified degree of tolerance, accommodating predictions that are close to the correct class. Formally, it is defined as: $CAP_{\pm k}(y, \hat{y}) = \frac{1}{n} \sum_{i=1}^n \mathbb{I}(|y_i - \hat{y}_i| \leq k)$, where y represents the vector of true class labels, \hat{y} denotes

the model’s predictions, k specifies the tolerance level (e.g., ± 1 or ± 2 classes), n is the total number of samples, and $\mathbb{I}(\cdot)$ is the indicator function that evaluates to 1 if the condition is met and 0 otherwise. This metric thus quantifies the proportion of samples where the model’s predictions fall within the allowed tolerance around the true class.

Figure 4(a) shows the scatter plot for predictions from the model trained using $T = 0.1$ -second window images, while Figure 4(b) displays results for the $T = 0.3$ -second window. The test dataset includes 12,520 traces with an average of 21.2 images per trace for $T = 0.1$ seconds, and 12,142 traces with an average of 7.5 images per trace for $T = 0.3$ seconds.

The figures highlight significant differences in performance between the two models. The $T = 0.3$ -second model has 71% of predictions within ± 3 (CAP) of the true values, whereas the $T = 0.1$ -second model achieves 92.6%, demonstrating a nearly 20% improvement in accuracy. We use a ± 3 tolerance level because, for both window lengths, the points represent aggregated prediction sums and, thus, aggregated errors. Additionally, the predictions of the model trained using a $T = 0.1$ -second window are more closely aligned along the diagonal, showing less deviation compared to those of the $T = 0.3$ -second model, suggesting that finer timing resolutions enhance cumulative prediction performance.

Figures 4(a) and 4(b) illustrate notable differences in predictive behavior between models trained and evaluated with $T = 0.3$ -second and $T = 0.1$ -second window sizes. Specifically, diagonal patterns appear in the predictions of the $T = 0.3$ -second model that are absent in the $T = 0.1$ -second model’s predictions. This phenomenon exists for several reasons. When using a $T = 0.1$ subdivision, a high percentage of images have lower class values, and the model trained on this dataset is very accurate for low-value classes. In contrast, a $T = 0.3$ subdivision yields images with higher class values, increasing the variance of the true labels, and both models perform worse for higher-value classes compared to lower-value ones. Additionally, any incorrect prediction by either model contributes to an increase in the cumulative predictions for the remainder of the trace, thereby elevating the overall predicted values. The $T = 0.1$ -second model’s box plot is presented in Appendix ..

5 Conclusion

In this paper, we introduced *VisQUIC*, an openly available dataset comprising labeled QUIC traffic traces along with their corresponding SSL keys. By providing both the encrypted traffic and the SSL keys, *VisQUIC* enables unprecedented analysis of QUIC and HTTP/3 communications at a granular level. This dataset serves as a valuable resource for researchers aiming to develop advanced network analysis tools, enhance intrusion detection systems, and optimize

network performance. To demonstrate the dataset’s potential, we transformed QUIC connection data into sequences of RGB images and applied deep learning models to predict network traffic characteristics. Our results showcased high accuracy with up to 97% CAP accuracy, in predicting HTTP/3 responses and analyzing traffic patterns, underscoring the versatility of *VisQUIC* in supporting ML applications for network traffic analysis. By releasing *VisQUIC* with detailed traces and SSL keys, we aim to facilitate further research into encrypted traffic analysis and drive innovation in both networking and ML domains.

A Appendices

The dataset comprises traces from sequential web page requests performed one at a time. A page request workload was chosen due to the limited number of web servers streaming video over QUIC, which restricts server-side traffic diversity. Unlike page requests, video streaming traffic is heavily influenced by server-side streaming algorithms rather than network conditions. Future work should examine varying bandwidth conditions and include traces collected using not only Chrome.

A.1 Dedicated Loss Function

To demonstrate *VisQUIC*, we model the estimation of HTTP/3 responses in a QUIC connection as a discrete regression problem and implemented the following loss function:

$L = \alpha \text{FL} + (1 - \alpha) ((\beta \text{ORL} + (1 - \beta) \text{DBL})$. It comprises an aggregate of three terms: (1) a *focused loss* (FL) term, intended to alleviate class imbalance by minimizing the relative loss for well-classified cases while emphasizing difficult-to-classify ones; (2) a *distance-based loss* (DBL) term penalizing the model according to the predicted class’s distance from the true label; and (3) an *ordinal regression loss* (ORL) term that introduces higher penalties for misclassifications that disrupt the natural ordinal sequence of the dataset, where lower class values occur more frequently.

The FL term [15] builds on the weighted cross-entropy loss [7] by adding a focusing parameter, γ , which adjusts the influence of each sample on the training process based on the classification confidence. Specifically, FL scales the loss by $(1 - p_t)^\gamma$, where p_t is the predicted probability of the true class y . This scaling reduces the loss from easy examples (where p_t is high), thereby increasing it for hard, misclassified examples, focusing training efforts on samples where improvement is most needed. Accordingly, the term is: $\text{FL}(\mathbf{x}, \mathbf{y}) = \mathbb{E}_{(\mathbf{x}, \mathbf{y})} [-w(y) \cdot (1 - \hat{y}_y(\mathbf{x}))^\gamma \cdot \mathbf{y}^T \log \hat{\mathbf{y}}(\mathbf{x})]$, where \mathbf{x} denotes the input sample, \mathbf{y} is the one-hot encoded ground truth label, $\hat{\mathbf{y}}(\mathbf{x})$ represents the model’s output of class probabilities, $\hat{y}_y(\mathbf{x})$ denotes the predicted probability of the true class y , and $w(y)$ is a weight inversely proportional to the class frequency of y in the training dataset. By assigning a higher

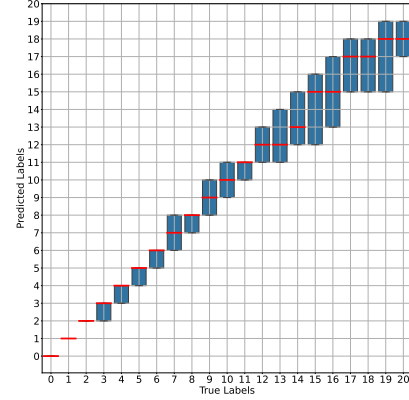


Figure 5: Prediction errors assuming known web servers using the $T = 0.1$ model. Red lines indicate the median predicted value.

weight to less frequent classes, the model places more emphasis on accurately classifying these classes during training. It is an effective strategy for dealing with class imbalance [2, 15]. FL thus minimizes the relative loss for well-classified examples, while emphasizing difficult-to-classify ones. The DBL term [25] is: $\text{DBL} = \mathbb{E}_{(\mathbf{x}, \mathbf{y})} [\sum_i \hat{y}_i(\mathbf{x}) \cdot |i - y|]$, where y is the ground truth class. DBL penalizes predictions based on the absolute difference between the predicted class indices and the true label.

Finally, the ORL term [9, 13] is:

$\text{ORL} = \mathbb{E}_{(\mathbf{x}, \mathbf{y})} [-\mathbf{y}^T \log \sigma(\hat{\mathbf{y}}) - (1 - \mathbf{y})^T \log \sigma(-\hat{\mathbf{y}})]$, with σ denoting the sigmoid function saturating the input between 0 and 1. ORL uses a binary cross-entropy loss function, which compares the activation of each output neuron to a target that shows if the true class is greater than or equal to each class index, thus helping the model determine the order of the classes. Both DBL and ORL consider the relations between classes; they do so in different ways: DBL penalizes predictions based on the numerical distance, while ORL makes explicit use of the classes’ order. It focuses on preserving the correct order among predictions rather than the numerical distance between them.

The parameters α , β , and γ balance the contributions of the loss components. Specifically, α controls the weight between the FL term and the combination of ORL and DBL, where a higher α emphasizes FL and a lower α favors ORL and DBL. The parameter β adjusts the balance between ORL and DBL, assigning more weight to ORL with higher β and to DBL with lower β . Lastly, γ modulates the focusing effect within the FL term; a higher γ intensifies the focus on difficult, misclassified examples—beneficial in highly imbalanced scenarios—while a lower γ reduces this effect, making FL resemble standard cross-entropy loss with uniformly weighted misclassifications.

A.2 Additional Evaluation:

Figure 5 presents a box plot of class prediction accuracy on out-of-training sample traces with a window length of $T = 0.1$ seconds. The horizontal axis denotes the true labels, while the vertical axis displays the predicted labels, with each box representing the 25-th, 50-th, and 75-th percentiles. For lower-value classes (0, 1, and 2), the boxes appear as single lines, indicating consistent predictions close to the true values.

References

- [1] Sultan Almuhammadi, Abdullatif Alnajim, and Mohammed Ayub. 2023. QUIC Network Traffic Classification Using Ensemble Machine Learning Techniques. *Applied Sciences* 13, 8 (2023), 4725.
- [2] Yuri Sousa Aurelio, Gustavo Matheus De Almeida, Cristiano Leite de Castro, and Antonio Padua Braga. 2019. Learning from imbalanced data sets with weighted cross-entropy function. *Neural processing letters* 50 (2019), 1937–1949.
- [3] Mike Bishop. 2022. HTTP/3. RFC 9114. <https://doi.org/10.17487/RFC9114>
- [4] CAIDA. 2024. The CAIDA Passive Monitored Traces Dataset. https://www.caida.org/catalog/datasets/passive_dataset/. Accessed: 2024-05-30.
- [5] Efstratios Chatzoglou, Vasileios Kouliaridis, and Georgios Kambourakis. 2023. A hands-on gaze on HTTP/3 security through the lens of HTTP/2 and a public dataset. *Computers and Security* 125 (2023), 103051. <https://doi.org/10.1016/j.cose.2022.103051>
- [6] chromium. 2017. chromium. <https://chromium.googlesource.com/chromium/src/+lkgr/headless/>
- [7] Pieter-Tjerk De Boer, Dirk P Kroese, Shie Mannor, and Reuven Y Rubinstein. 2005. A tutorial on the cross-entropy method. *Annals of operations research* 134 (2005), 19–67.
- [8] Yasir Ali Farrukh, Syed Wali, Irfan Khan, and Nathaniel D Bastian. 2023. Senet-i: An approach for detecting network intrusions through serialized network traffic images. *Engineering Applications of Artificial Intelligence* 126 (2023), 107169.
- [9] Eibe Frank and Mark Hall. 2001. A simple approach to ordinal classification, In Machine Learning: ECML 2001: 12th European Conference on Machine Learning Freiburg, Germany, September 5–7, 2001 Proceedings 12. *ECML 2001*, 145–156.
- [10] Ray J Frank, Neil Davey, and Stephen P Hunt. 2001. Time series prediction and neural networks. *Journal of intelligent and robotic systems* 31 (2001), 91–103.
- [11] Sergei Golubev and Evgenia Novikova. 2022. Image-based Intrusion Detection in Network Traffic. In *International Symposium on Intelligent and Distributed Computing*. Springer, 51–60.
- [12] Florian Gratzner, Sebastian Gallenmüller, and Quirin Scheitle. 2016. Quic-quick udp internet connections. *Future Internet and Innovative Internet Technologies and Mobile Communications* (2016).
- [13] Ralf Herbrich, Thore Graepel, and Klaus Obermayer. 1999. Support vector learning for ordinal regression. *IEEE* (1999).
- [14] Diederik P Kingma and Jimmy Ba. 2014. Adam: A method for stochastic optimization. *arXiv preprint arXiv:1412.6980* (2014).
- [15] Tsung-Yi Lin, Priya Goyal, Ross Girshick, Kaiming He, and Piotr Dollár. 2017. Focal loss for dense object detection. In *Proceedings of the IEEE international conference on computer vision*. IEEE, 2980–2988.
- [16] Jan Luxemburk, Karel Hynek, Tomáš Čejka, Andrej Lukačovič, and Pavel Šiška. 2023. CESNET-QUIC22: A large one-month QUIC network traffic dataset from backbone lines. *Data in Brief* 46 (2023), 108888.
- [17] Kiran Maharana, Surajit Mondal, and Bhushankumar Nemade. 2022. A review: Data pre-processing and data augmentation techniques. *Global Transitions Proceedings* 3, 1 (2022), 91–99.
- [18] Borja Merino. 2013. *Instant traffic analysis with Tshark how-to*. Packt Publishing Ltd.
- [19] Robert J. Shahla, Reuven Cohen, and Friedman Roy. 2024. Traffic-Grinder: A 0-RTT-Aware QUIC Load Balancer. In *2024 IEEE 32st International Conference on Network Protocols (ICNP)*. IEEE.
- [20] Tal Shapira and Yuval Shavitt. 2019. Flowpic: Encrypted internet traffic classification is as easy as image recognition. In *IEEE INFOCOM 2019-IEEE Conference on Computer Communications Workshops (INFOCOM WKSHPS)*. IEEE, 680–687.
- [21] Jean-Pierre Smith. 2021. Website Fingerprinting in the Age of QUIC. 2021 (2021).
- [22] statcounter. 2023. Browser Market Share Worldwide. StatCounter Global Stats. <https://gs.statcounter.com/browser-market-share> (accessed October 2023).
- [23] Shun Tobiyama, Yukiko Yamaguchi, Hajime Shimada, Tomonori Ikuse, and Takeshi Yagi. 2016. Malware detection with deep neural network using process behavior. In *2016 IEEE 40th annual computer software and applications conference (COMPSAC)*, Vol. 2. IEEE, 577–582.
- [24] Petr Velan, Milan Čermák, Pavel Čeleda, and Martin Drašar. 2015. A survey of methods for encrypted traffic classification and analysis. *International Journal of Network Management* 25, 5 (2015), 355–374.
- [25] Qi Wang, Yue Ma, Kun Zhao, and Yingjie Tian. 2020. A comprehensive survey of loss functions in machine learning. *Annals of Data Science* (2020), 1–26.